Title: **Systematic detection of divergent brain protein-coding genes in human evolution and their roles in cognition**

Short title: **Divergent brain protein-coding genes in human evolution**

Guillaume Dumas[a], Simon Malesys[a] and Thomas Bourgeron[a]

[a] Human Genetics and Cognitive Functions, Institut Pasteur, UMR3571 CNRS, Université de Paris, Paris, (75015) France

Corresponding author:

Guillaume Dumas

Human Genetics and Cognitive Functions

Institut Pasteur

75015 Paris, France

Phone: +33 6 28 25 56 65

guillaume.dumas@pasteur.fr

Abstract

The human brain differs from that of other primates, but the genetic basis of these differences remains unclear. We investigated the evolutionary pressures acting on almost all human protein-coding genes (*N*=11,667; 1:1 orthologs in primates) on the basis of their divergence from those of early hominins, such as Neanderthals, and non-human primates. We confirm that genes encoding brain-related proteins are among the most strongly conserved protein-coding genes in the human genome. Combining our evolutionary pressure metrics for the protein-coding genome with recent datasets, we found that this conservation applied to genes functionally associated with the synapse and expressed in brain structures such as the prefrontal cortex and the cerebellum. Conversely, several of the protein-coding genes that diverge most in hominins relative to other primates are associated with brain-associated diseases, such as micro/macrocephaly, dyslexia, and autism. We also showed that cerebellum granule neurons express a set of divergent protein-coding genes that may have contributed to the emergence of fine motor skills and social cognition in humans. This resource is available from http://neanderthal.pasteur.fr and can be used to estimate evolutionary constraints acting on a set of genes and to explore their relative contributions to human traits.

Introduction

Modern humans (*Homo sapiens*) can perform complex cognitive tasks well and communicate with their peers [1]. Anatomic differences between the brains of humans and other primates are well documented (e.g. cortex size, prefrontal white matter thickness, lateralization), but the way in which the human brain evolved remains a matter of debate [2]. A recent study of endocranial casts of *Homo sapiens* fossils indicates that, brain size in early *Homo sapiens*, 300,000 years ago, was already within the range of that in present-day humans [3]. However, brain shape, evolved more gradually within the *Homo sapiens* lineage, reaching its current form between about 100,000 and 35,000 years ago. It has also been suggested that the enlargement of the prefrontal cortex relative to the motor cortex in humans is mirrored in the cerebellum by an enlargement of the regions of the cerebellum connected to the prefrontal cortex [4]. These anatomic processes of tandem evolution in the brain paralleled the emergence of motor and cognitive abilities, such as bipedalism, planning, language, and social awareness, which are particularly well developed in humans.

Genetic differences in primates undoubtedly contributed to these brain and cognitive differences, but the genes or variants involved remain largely unknown. Indeed, demonstrating that a genetic variant is adaptive requires strong evidence at both the genetic and functional levels. Only few genes have been shown to be human-specific. They include *SRGAP2C* [5], *ARHGAP11B* [6] and *NOTCH2NL* [7], which emerged through recent gene duplication in the *Homo* lineage [8]. Remarkably, the expression of these human specific genes in the mouse brain expand cortical neurogenesis [6,7,9,10]. Several genes involved in brain function have been shown to display accelerated coding region evolution in humans. For example, *FOXP2* has been associated with verbal apraxia and *ASPM* with microcephaly [11,12]. Functional studies have also shown that mice carrying a “humanized” version of *FOXP2* display qualitative changes in ultrasonic vocalization [13]. However, these reports

58 targeting only specific genes sometimes provide contradictory results [14]. Other studies
59 have reported sequence conservation to be stronger in the protein-coding genes of the brain
60 than in those of other tissues [15–17], suggesting that the main substrate of evolution in the
61 brain is regulatory changes in gene expression [18–20] and splicing [21]. In addition, several
62 recent studies have recently explored the genes subjected to the highest degrees of constraint
63 during primate evolution or in human populations, to improve estimations of the
64 pathogenicity of variants identified in patients with genetic disorders [22,23]. By contrast,
65 few studies have systematically detected genes that have diverged during primate evolution
66 [24,25].

67 We describe here an exhaustive screening of all protein-coding genes for conservation
68 and divergence from the common primate ancestor, making use of rich datasets of brain
69 single-cell transcriptomics, proteomics and imaging to investigate the relationships between
70 these genes and brain structure, function, and diseases.

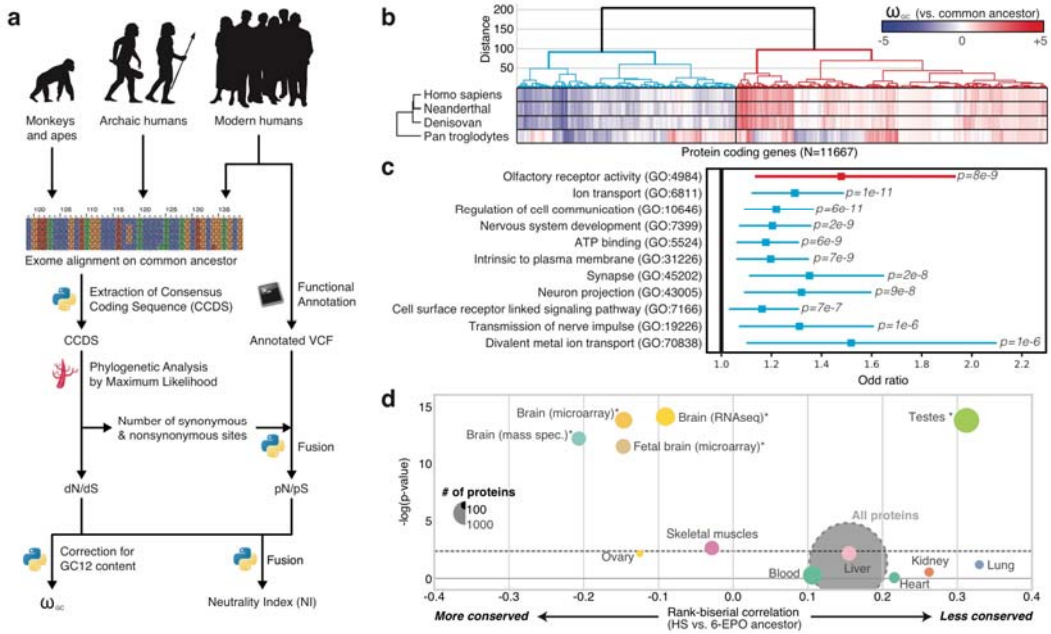

Figure 1 Evolution of protein-coding genes across tissues and biological functions. (a) Analysis pipeline for the extraction of ω_{GC12}, a corrected and normalized measurement of evolution of protein-coding genes that behaves like a Z-score and takes into account the GC content of codons. (b) Hierarchical clustering, on the basis of ω_{GC12}, across all protein-coding genes (1:1 orthologs in hominins with medium coverage; See Supplementary Table 1). (c) Gene ontology (GO) enrichments for the red and blue clusters in panel b (See Supplementary Table 2 for all GO terms). Horizontal lines indicate the 95% confidence intervals. (d) Funnel plot summarizing the evolution of protein-coding genes specifically expressed in different tissues of the human body (Supplementary Table 3). The dashed horizontal line indicates the threshold for significance after Bonferroni correction. Stars indicate the set of genes for which statistical significance was achieved in multiple comparisons after correction, with a bootstrap taking GC12 content and coding sequence length into account. HS: *Homo sapiens*; 6-EPO ancestor: the reconstructed ancestral genome of primates based on alignments of human, chimpanzee, gorilla, orangutan, rhesus macaque, and marmoset genomes.

Results

Strong conservation of brain protein-coding genes

We first compared the sequences of modern humans, archaic humans, and other primates to those of their common primate ancestor (inferred from the Compara 6-way primate Enredo, Pecan, Ortheus multiple alignments [26]), to extract a measurement of evolution for 11,667 of the 1:1 orthologs across primates, selected from the 17,808 protein-coding genes in the modern human genome (Fig. 1a, see also Supplementary Fig. 1 and 2; 27). This resource is available online from http://neanderthal.pasteur.fr. Our measurement is derived from one of the most widely used and reliable measurements of evolutionary pressure on protein-coding regions, the dN/dS ratio [28], also called ω. This measurement compares the rates of non-synonymous and synonymous mutations of coding sequences. If there are more non-synonymous mutations than expected, there is divergence, if fewer, there is conservation. We first estimated dN and dS for all 1:1 orthologous genes, because the evolutionary constraints on duplicated genes are relaxed [29] (note: only the Y chromosome was excluded from these analyses). We then adjusted the dN/dS ratio for biases induced by variations of mutations rate with the GC content of codons. Finally, we renormalized the values obtained for each taxon across the whole genome. The final ω_{GC12} obtained took the form of Z-score corrected for GC content that quantified the unbiased divergence of genes relative to the ancestral primate genome [27].

Using the ω_{GC12} for all protein-coding genes in *Homo sapiens*, Denisovans, Neanderthals, and *Pan troglodytes*, we identified two distinct clusters in hominins (Fig. 1b and Supplementary Table 1): one containing divergent protein-coding genes, enriched in olfactory genes (OR=1.48, p=8.4e-9), and one with conserved protein-coding genes, enriched in brain-related biological functions (Fig. 1c and Supplementary Table 2). This second cluster

112 revealed a particularly strong conservation of genes encoding proteins involved in nervous
113 system development (OR=1.2, *p*=2.4e-9) and synaptic transmission (OR=1.35, *p*=1.7e-8).

114 We investigated the possible enrichment of specific tissues in conserved and
115 divergent proteins by analyzing RNAseq (Illumina Bodymap2 and GTEx), microarray and
116 proteomics datasets (Methods). For expression data, we evaluated the specificity of genes by
117 normalizing their profile across tissues (Supplementary Fig. 3). The results confirmed a
118 higher degree of conservation for protein-coding genes expressed in the brain (Wilcoxon rank
119 correlation (rc)=-0.1, *p*=4.1e-12, bootstrap corrected for gene length and GC content) than for
120 those expressed elsewhere in the body, with the greatest divergence observed for genes
121 expressed in the testis (Wilcoxon rc=0.3, *p*=7.8e-11, bootstrap corrected for gene length and
122 GC content; Fig. 1d, see also Supplementary Fig. 4 and 5). This conservation of brain
123 protein-coding genes was replicated with two other datasets (MicroArray: Wilcoxon OR=-
124 0.18, *p*=1.8e-12; mass spectrometry: Wilcoxon rc=-0.21, *p*=1.55e-9; bootstrap corrected for
125 gene length and GC content).

126

127 **Conservation of protein-coding genes relating to nervous system substructure and**
128 **neuronal functions**

129 We then used microarray [30] and RNAseq [31] data to investigate the evolutionary pressures
130 acting on different regions of the central nervous system. Three central nervous system
131 substructures appeared to have evolved under the highest level of purifying selection at the
132 protein sequence level (ω_{GC12}<2, i.e. highly conserved): (i) the cerebellum (Wilcoxon rc=-
133 0.29, *p*=5.5e-6, Bonferroni corrected) and the cerebellar peduncle (Wilcoxon rc=-0.11,
134 *p*=3.2e-4, bootstrap corrected for gene length and GC content), (ii) the amygdala (Wilcoxon
135 rc=-0.11, *p*=4.1e-6, bootstrap corrected for gene length and GC content), and, more

surprisingly, (iii) the prefrontal cortex (Wilcoxon rc=-0.1, *p*=5.7e-10, bootstrap corrected for gene length and GC content; Fig. 2a, see also Supplementary Table 3). Indeed, it has been suggested that the prefrontal cortex is one of the most divergent brain structure in human evolution [32], this diversity being associated with high-level cognitive function [33]. Only one brain structure was more divergent than expected: the superior cervical ganglion (Wilcoxon rc=0.22, *p*=1e-6, bootstrap corrected for gene length and GC content). This structure provides sympathetic innervation to many organs and is associated with the archaic functions of fight-or-flight response. The divergent genes expressed in the superior cervical ganglion include *CARF*, which was found to be specifically divergent in the genus *Homo*. This gene encodes a calcium-responsive transcription factor that regulates the neuronal activity-dependent expression of *BDNF* [34] and a set of singing-induced genes in the song nuclei of the zebra finch, a songbird capable of vocal learning [35]. This gene had a raw dN/dS of 2.44 (7 non-synonymous vs 1 synonymous mutations in *Homo sapiens* compared to the common primate ancestor) and was found to be one of the most divergent protein-coding genes expressed in the human brain.

We then investigated the possible enrichment of conserved and divergent genes in brain-specific gene ontology terms. All pathways displayed high overall levels of conservation, but genes encoding proteins involved in glutamatergic and GABAergic neurotransmission were generally more conserved (Wilcoxon rc=-0.25; *p*=9.8e-6, Bonferroni corrected) than those encoding proteins involved in dopamine and peptide neurotransmission and intracellular trafficking (Fig. 2b, see also Supplementary Fig. 6 and Supplementary Table 3). The recently released ontology of the synapse provided by the SynGO consortium (http://syngoportal.org) was incorporated into this analysis, not only confirming the globally strong conservation of the synapse, but also revealing its close relationship to trans-synaptic signaling processes (Wilcoxon rc=-0.21, p=4.5e-5, Bonferroni corrected) and to postsynaptic

161 (rc=-0.56, p=6.3e-8, Bonferroni corrected) and presynaptic membranes (Wilcoxon: rc=-0.56,
162 *p*=7e-8, Bonferroni corrected ; Fig. 2c,d).

163

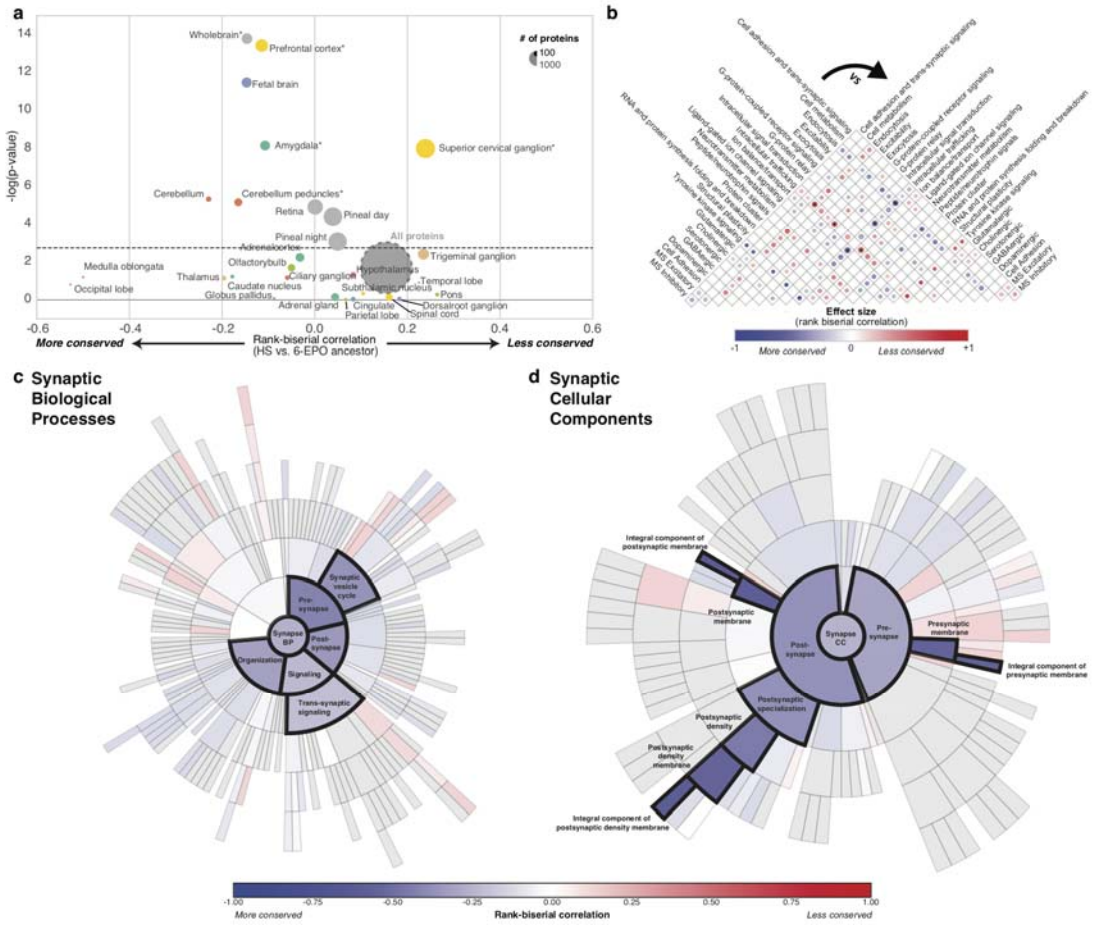

164

165 **Figure 2 Evolution of brain-related protein-coding genes. (a) Funnel plot summarizing**
166 **the evolution of protein-coding genes specifically expressed in brain substructures; the**
167 **dashed horizontal line indicates the threshold for significance after Bonferroni**
168 **correction. Stars indicate sets of genes for which statistical significance was achieved for**
169 **multiple comparisons with bootstrap correction; (b) Matrix summarizing the effect size**
170 **of the difference in protein-coding gene divergence between synaptic functions; colored**
171 **cells indicate Mann-Whitney comparisons with a nominal *p*-value <0.05. Black dots**
172 **indicate comparisons satisfying the Bonferroni threshold for statistical significance. (c,**

d) SynGO sunburst plots showing nested statistically conserved (blue) biological processes and cellular components of the synapse.

Divergent protein-coding genes and their correlation with brain expression and function

We focused on the genes situated at the extremes of the ω_{GC12} distribution (>2SD; Fig. 3a; Supplementary Table 4) and those fixed in the modern *Homo sapiens* population (neutrality index<1), to ensure that we analyzed the most-divergent protein-coding genes. Only 126 of these 352 highly divergent protein-coding genes were brain-related (impoverishment for brain genes, Fisher's exact test OR=0.66, p=1e-4), listed as synaptic genes [36,37], specifically expressed in the brain (+2SD for specific expression) or related to a brain disease (extracted systematically from Online Mendelian Inheritance in Man - OMIM: https://www.omim.org and Human Phenotype Ontology - HPO: https://hpo.jax.org/app/). For comparison, we also extracted the 427 most strongly conserved protein-coding genes, 290 of which were related to the brain categories listed above (enrichment for brain genes, Fisher's exact test OR=1.26, p=0.0032).

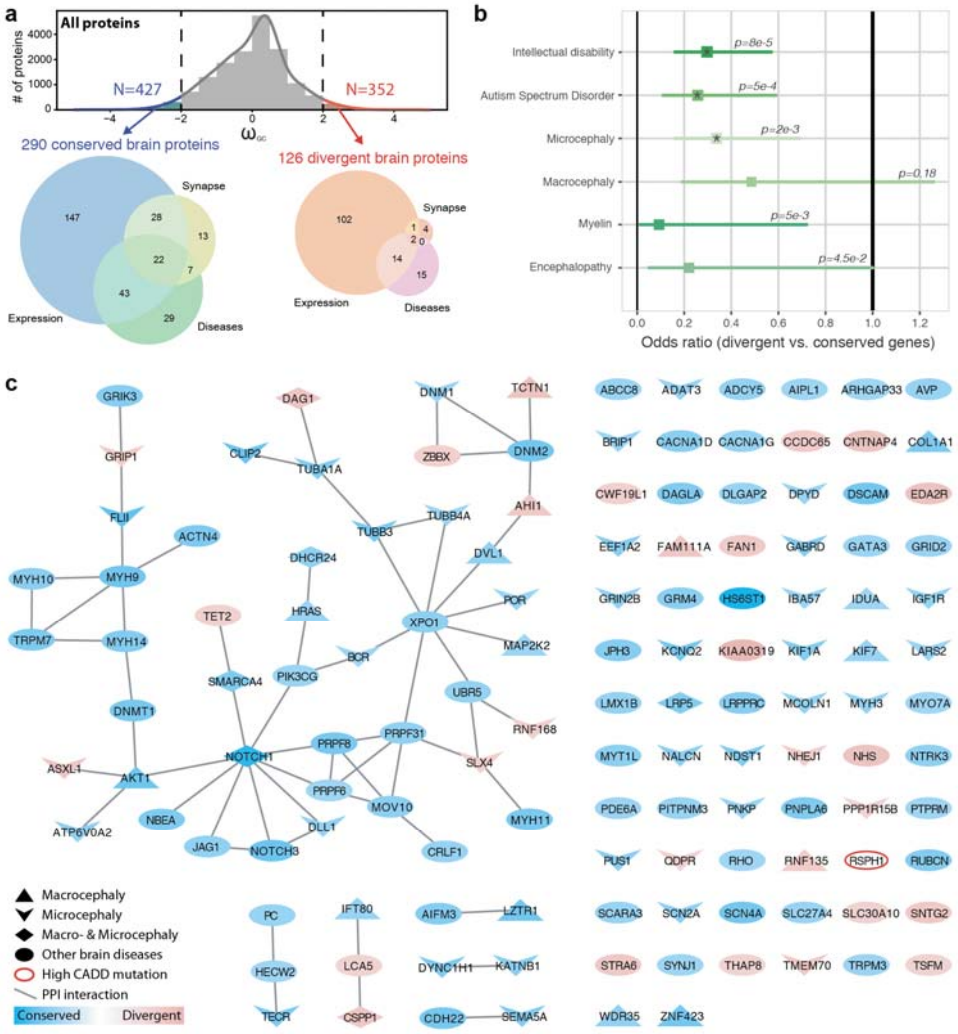

Figure 3 Brain protein-coding genes and human diseases. (a) Distribution of ω_{GC12} and Venn diagrams describing the most conserved and divergent protein-coding genes specifically expressed in the brain, related to the synapse, or brain diseases (Supplementary Table 4). (b) Odds ratios for protein-coding gene sets related to brain diseases (Fisher's exact test; Asterisks indicate *p*-values significant after Bonferroni correction; horizontal lines indicate 95% confidence intervals) (c) Protein-protein interaction (PPI) network for the most conserved and divergent protein-coding genes associated with brain diseases. The *RSPH1* gene has accumulated variants with a high combined annotation-dependent depletion (CADD) score, which estimates the deleteriousness of a genetic variant.

Using these 427 highly conserved and 352 highly divergent genes, we first used the Brainspan data available from the specific expression analysis (SEA) to confirm that the population of genes expressed in the cerebellum and the cortex was enriched in conserved genes (Supplementary Figure 7). Despite this conservation, based on the adult Allen Brain atlas, we identified a cluster of brain subregions (within the hypothalamus, cerebral nuclei, and cerebellum) more specifically expressing highly divergent genes (Supplementary Figure 8). Analyses of the prenatal human brain laser microdissection microarray dataset [38] also revealed an excess of divergent protein-coding genes expressed in the medial ganglionic eminence (MGE; OR=2.78[1.05, 7.34], p=0.039; Supplementary Table 5) which is implicated in production of GABAergic interneurons and their migration to neocortex during development [39].

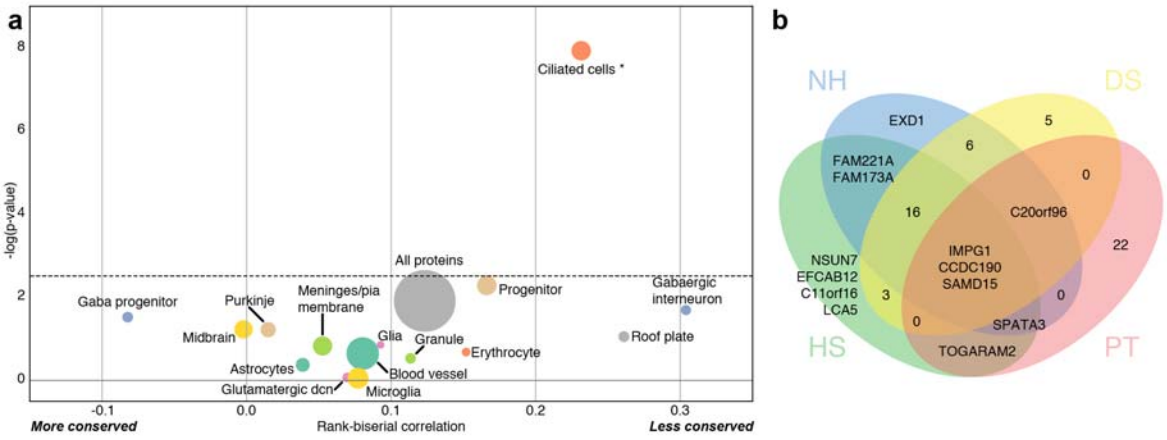

Figure 4 Evolution of protein-coding genes expressed in different cerebellum cell types. (a) Funnel plot summarizing the evolution of protein-coding genes specifically expressed in different cell types within the cerebellum (Supplementary Table 6). (b) Venn diagram summarizing the divergent protein-coding genes of *Homo sapiens* (HS), Neanderthals (NH), Denisovans (DS), and *Pan troglodytes* (PT) specifically expressed in Cluster 47, so-called "ciliated cells" [40].

219

220 In single-cell transcriptomic studies of the mouse cerebellum [40,41], we found that cells
221 expressing cilium marker genes, such as *DYNLRB2* and *MEIG1*, were the principal cells with
222 higher levels of expression of the most divergent protein-coding genes (after stringent
223 Bonferroni and bootstrap correction for gene length and GC content, Fig. 4a). Those "ciliated
224 cells" were not anatomically identified in the cerebellum [40], but their associated cilium
225 markers were found to be expressed at the site of the cerebellar granule cells [42]. These cells
226 may, therefore, be a subtype of granule neurons involved in cerebellar function. The most
227 divergent proteins in these ciliated cells code for the tubulin tyrosine ligase like 6 (TTLL6),
228 the DNA topoisomerase III alpha (TOP3A), the dynein cytoplasmic 2 light intermediate
229 chain 1 (DYNC2LI1*)* and the lebercilin (LCA5) localized to the axoneme of ciliated cells.
230 Given that most protein coding divergence occurs in testes and that the flagella of sperm and
231 cilia of other cells are structurally related, is it possible that the enrichment of ciliated cells
232 among the most divergent genes could be another feature of testis rather than brain
233 divergence. However, only *TTLL6* is highly expressed in testes, suggesting a neural relevance
234 for *DYNC2LI1*, *LCA5*, and *TOP3A*. Interestingly, some of these protein coding genes are also
235 involved in human brain-related ciliopathies such as Joubert syndrome [43] and microcephaly
236 (see below). A similar single-cell transcriptomic analysis of the human cerebral cortex [41]
237 revealed no such strong divergent pattern in any cell type (Supplementary Figure 9).

238 Finally, we assessed the potential association with brain functions, by extracting 19,244 brain
239 imaging results from 315 fMRI-BOLD studies (T and Z score maps; see Supplementary
240 Table 7 for the complete list) from NeuroVault [44] and comparing the spatial patterns
241 observed with the patterns of gene expression in the Allen Brain atlas [45,46]. The
242 correlation between brain activity and divergent gene expression was stronger in subcortical
243 structures than in the cortex (Wilcoxon rc=0.14, p=2.5e-248). The brain activity maps that

correlate with the expression pattern of the divergent genes (see Supplementary Table 8 for details) were enriched in social tasks (empathy, emotion recognition, theory of mind, language; Fisher's exact test p=2.9e-20, OR=1.72, $CI_{95\%}$=[1.53, 1.93]; see Supplementary Figure 10 for illustration).

Divergent protein-coding genes and their relationship to brain disorders

Our systematic analysis revealed that highly constrained protein-coding genes were more associated with brain diseases or traits than divergent protein-coding genes, particularly for microcephaly (p=0.002, OR=0.37, $CI_{95\%}$=[0.16, 0.69], Bonferroni-corrected), intellectual disability (p=7.91e-05, OR=0.30 $CI_{95\%}$=[0.16, 0.57], Bonferroni-corrected) and autism (p=0.0005, OR=0.26, $CI_{95\%}$=[0.11, 0.59], Bonferroni-corrected) and for diseases associated with myelin (Fisher's exact test p=0.005, OR=0.09, $CI_{95\%}$=[0.01, 0.72], uncorrected) and encephalopathy (Fisher's exact test p=0.045, OR=0.22, $CI_{95\%}$=[0.05, 1.0], uncorrected; Figure 3b). The highly conserved protein-coding genes associated with brain diseases included those encoding tubulins (TUBA1A, TUBB3, TUBB4A), dynamin (DNM1), chromatin remodeling proteins (SMARCA4) and signaling molecules, such as AKT1, DVL1, NOTCH1 and its ligand DLL1, which were associated with neurodevelopmental disorders of different types (Supplementary Table 4). We also identified 31 highly divergent protein-coding genes associated (based on OMIM and HPO data) with several human diseases or conditions, such as micro/macrocephaly, autism or dyslexia.

A comparison of humans and chimpanzees with our common primate ancestor revealed several protein-coding genes associated with micro/macrocephaly with different patterns of evolution in humans and chimpanzees (Fig. 5). Some genes displayed a divergence specifically in the hominin lineage (*AHI1*, *ASXL1*, *CSPP1*, *DAG1*, *FAM111A*, *GRIP1*, *NHEJ1*, *QDPR*, *RNF135*, *RNF168*, *SLX4*, *TCTN1*, and *TMEM70*) or in the chimpanzee (*ARHGAP31*, *ATRIP*, *CPT2*, *CTC1*, *HDAC6*, *HEXB*, *KIF2A*, *MKKS*, *MRPS22*,

269 *RFT1*, *TBX6*, and *WWOX*). The *PPP1R15B* phosphatase gene associated with microcephaly
270 diverged from the common primate ancestor in both taxa. None of the genes related to
271 micro/macrocephaly was divergent only in *Homo sapiens* (Fig. 5).

272

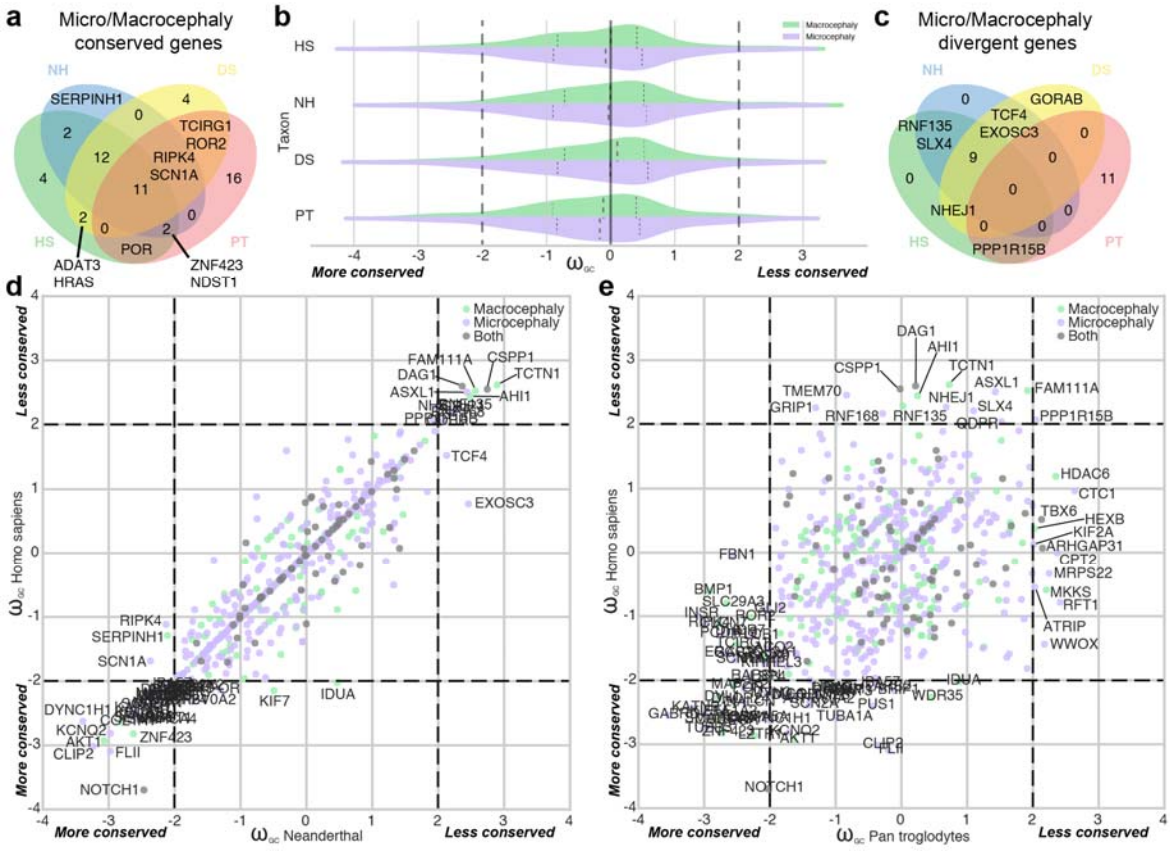

273

274 **Figure 5. Evolution of the protein-coding genes associated with micro- or macrocephaly**
275 **in humans. Comparison of ω_{GC12} across taxa for the microcephaly- and macrocephaly-**
276 **associated genes. Venn diagrams for the conserved (a) and divergent (c) protein-coding**
277 **genes for *Homo sapiens* (HS), Neanderthals (NH), Denisovans (DS), and *Pan troglodytes***
278 **(PT). (b) Violin plots of ω_{GC} for protein-coding genes associated with microcephaly**
279 **(purple), macrocephaly (green) or both (gray). Scatter plots of ω_{GC} for the same genes,**
280 **comparing *Homo sapiens* with either Neanderthals (d) or *Pan troglodytes* (e).**

281

We also identified divergent protein-coding genes associated with communication disorders (Fig. 3c), such as autism (*CNTNAP4*, *AHI1*, *FAN1*, *SNTG2* and *GRIP1*) and dyslexia (*KIAA0319*). Interestingly, these genes diverged from the common primate ancestor only in the hominin lineage, and were strongly conserved in all other taxa (Fig. 6). They all have roles relating to neuronal connectivity (neuronal migration and synaptogenesis) and, within the human brain, were more specifically expressed in the cerebellum, except for *GRIP1*, which was expressed almost exclusively in the cortex.

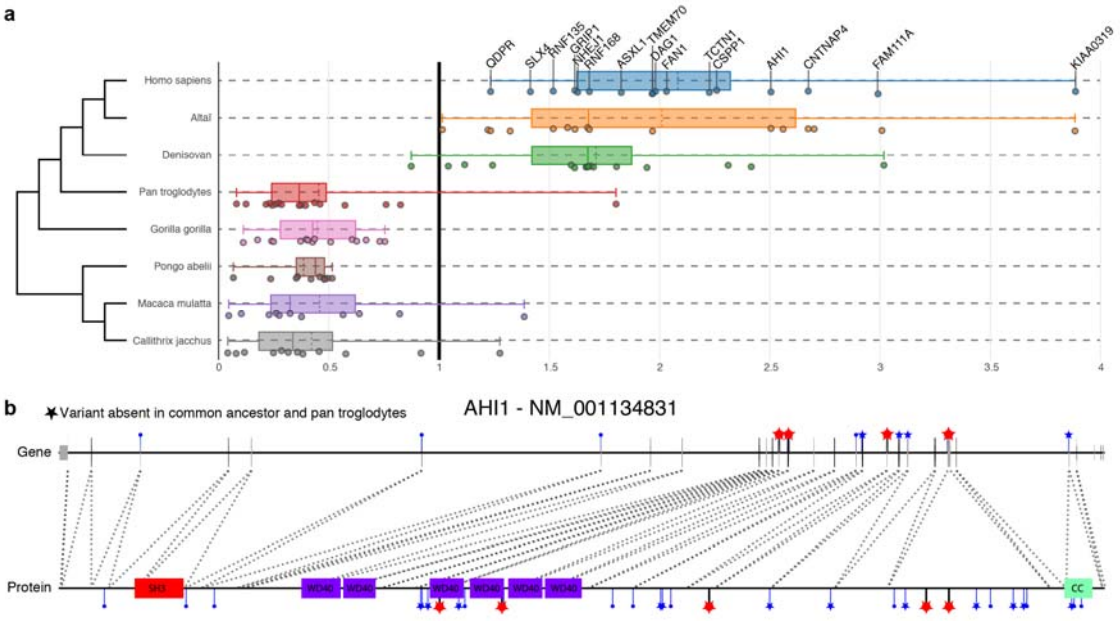

Figure 6. Examples of brain disorder-associated protein-coding genes displaying specific divergence in hominins during primate evolution. (a) Representation of 16 genes with dN/dS>1 in *Homo sapiens* and archaic hominins but dN/dS<1 for other primates. (b) Representation of hominin-specific variants of the *AHI1* gene, showing the correspondence with the protein; note how two variants lie within the WP40 functional domains. Red stars indicate variants (CADD>5) relative to the ancestor present in *Homo sapiens*, Neanderthals, and Denisovans, but not in *Pan troglodytes*.

298 The genes associated with autism include *CNTNAP4*, a member of the neurexin
299 protein family involved in correct neurotransmission in the dopaminergic and GABAergic
300 systems [47]. SNTG2 encodes a cytoplasmic peripheral membrane protein that binds to
301 NLGN3 and NLGN4X, two proteins associated with autism [48], and several copy-number
302 variants affecting *SNTG2* have been identified in patients with autism [49]. GRIP1 (glutamate
303 receptor-interacting protein 1) is also associated with microcephaly and encodes a synaptic
304 scaffolding protein that interacts with glutamate receptors. Variants of this gene have
305 repeatedly been associated with autism [50].

306 We also identified the dyslexia susceptibility gene *KIAA0319*, encoding a protein
307 involved in axon growth inhibition [51,52], as one of the most divergent brain protein-coding
308 genes in humans relative to the common primate ancestor (raw dN/dS=3.9; 9 non-
309 synonymous vs 1 synonymous mutations in *Homo sapiens* compared to the common primate
310 ancestor). The role of KIAA0319 in dyslexia remains a matter of debate, but its rapid
311 evolution in the hominoid lineage warrants further genetic and functional studies.

312 Finally, several genes display very high levels of divergence in *Homo sapiens*, but
313 their functions or association with disease remain unknown. For example, the zinc finger
314 protein ZNF491 (raw dN/dS=4.7; 14 non-synonymous vs 1 synonymous mutations in *Homo*
315 *sapiens* compared to the common primate ancestor) is specifically expressed in the
316 cerebellum and is structurally similar to a chromatin remodeling factor, but its biological role
317 remains to be determined. Another example is the *CCP110* gene, encoding a centrosomal
318 protein resembling ASPM, but not associated with a disease. Its function suggests that this
319 divergent protein-coding gene would be a compelling candidate for involvement in
320 microcephaly in humans. A complete list of the most conserved and divergent protein-coding
321 genes is available in Supplementary Table 4 and on the companion website.

Discussion

Divergent protein-coding genes and brain size in primates

Several protein-coding genes are thought to have played a major role in the increase in brain size in humans. Some of these genes, such as *ARHGAP11B, SRGAP2C* and *NOTCH2NL* [7], are specific to humans, having recently been duplicated [53]. Other studies have suggested that a high degree of divergence in genes involved in micro/macrocephaly may have contributed to the substantial change in brain size during primate evolution [24,54]. Several of these genes, such as *ASPM* [55] and *MCPH1* [56], seem to have evolved more rapidly in humans. However, the adaptive nature of the evolution of these genes has been called into question [57] and neither of these two genes were on the list of highly divergent protein-coding genes in our analysis (their raw dN/dS value are below 0.8).

Conversely, our systematic detection approach identified the most divergent protein-coding genes in humans for micro/macrocephaly, the top 10 such genes being *FAM111A, AHI1, CSPP1, TCTN1, DAG1, TMEM70, ASXL1, RNF168, NHEJ1, GRIP1*. This list of divergent protein-coding genes associated with micro/macrocephaly in humans can be used to select the best candidate human-specific gene/variants for further genetic and functional analyses, to improve estimates of their contribution to the emergence of anatomic difference between humans and other primates.

Some of these genes may have contributed to differences in brain size and to differences in other morphological features, such as skeleton development. For example, the divergent protein-coding genes *FAM111A* (raw dN/dS=2.99; 7 non-synonymous vs 1 synonymous mutations in *Homo sapiens* compared to the common primate ancestor) and *ASXL1* (raw dN/dS=1.83; 12 non-synonymous vs 3 synonymous mutations in *Homo sapiens* compared to the common primate ancestor) are associated with macrocephaly and

346 microcephaly, respectively. Patients with dominant mutations of *FAM111A* are diagnosed
347 with Kenny-Caffey syndrome (KCS). They display impaired skeletal development, with
348 small dense bones, short stature, primary hypoparathyroidism with hypocalcemia and a
349 prominent forehead [58]. The function of FAM111A remains largely unknown, but this
350 protein seems to be crucial to a pathway governing parathyroid hormone production, calcium
351 homeostasis, and skeletal development and growth. By contrast, patients with dominant
352 mutations of *ASXL1* are diagnosed with Bohring-Opitz syndrome, a malformation syndrome
353 characterized by severe intrauterine growth retardation, intellectual disability, trigonocephaly,
354 hirsutism, and flexion of the elbows and wrists with deviation of the wrists and
355 metacarpophalangeal joints [59]. *ASXL1* encodes a chromatin protein required to maintain
356 both the activation and silencing of homeotic genes.

357 Remarkably, three protein-coding genes (*AHI1*, *CSPP1* and *TCTN1*) in the top 5 of
358 the most divergent protein-coding genes, with raw dN/dS>2, are required for both cortical
359 and cerebellar development in humans. They are also associated with Joubert syndrome, a
360 recessive disease characterized by an agenesis of the cerebellar vermis and difficulties
361 coordinating movements. AHI1 is a positive modulator of classical WNT/ciliary signaling.
362 CSPP1 is involved in cell cycle-dependent microtubule organization and TCTN1 is a
363 regulator of Hedgehog during development.

364 *AHI1* was previously identified as a gene subject to positive selection during
365 evolution of the human lineage [60,61], but, to our knowledge, neither *CSPP1* nor *TCTN1*
366 has previously been described as a diverging during primate evolution. It has been suggested
367 that the accelerated evolution of *AHI1* required for ciliogenesis and axonal growth may have
368 played a role in the development of unique motor capabilities, such as bipedalism, in humans
369 [54]. Our findings provide further support for the accelerated evolution of a set of genes
370 associated with ciliogenesis. Indeed, we found that three additional genes involved in Joubert

371 syndrome, *CSPP1*, *TTLL6*, and *TCTN1*, were among the protein-coding genes that have
372 diverged most during human evolution, and our single-cell analysis revealed that ciliated
373 cells (a subtype of granule neurons) were the main category of cerebellar cells expressing
374 divergent genes.

375

376 **The possible link between a change in the genetic makeup of the cerebellum and the**
377 **evolution of human cognition**

378 The emergence of a large cortex was undoubtedly an important step for human cognition, but
379 other parts of the brain, such as the cerebellum, may also have made major contributions to
380 both motricity and cognition. In this study, we showed that the protein-coding genes
381 expressed in the cerebellum were among the most conserved in humans. However, we also
382 identified a set of divergent protein-coding genes with relatively strong expression in the
383 cerebellum and/or for which mutations affected cerebellar function. As discussed above,
384 several genes associated with Joubert syndrome, including *AHI1*, *CSPP1*, *TTLL6*, and
385 *TCTN1*, have diverged in humans and are important for cerebellar development. Furthermore,
386 the most divergent protein-coding genes expressed in the brain include *CNTNAP4*, *FAN1*,
387 *SNTG2*, and *KIAA0319*, which also display high levels of expression in the cerebellum and
388 have been associated with communication disorders, such as autism and dyslexia.

389 In humans, the cerebellum is associated with higher cognitive functions, such as
390 visuo-spatial skills, the planning of complex movements, procedural learning, attention
391 switching, and sensory discrimination [62]. It plays a key role in temporal processing [63]
392 and in the anticipation and control of behavior, through both implicit and explicit
393 mechanisms [62]. A change in the genetic makeup of the cerebellum would therefore be

394 expected to have been of great advantage for the emergence of the specific features of human
395 cognition.

396 Despite this possible link between the cerebellum and the emergence of human
397 cognition, much less attention has been paid to this part of the brain than to the cortex, on
398 which most of the functional studies investigating the role of human-specific genes/variants
399 have focused. For example, *SRGAP2C* expression is almost exclusively restricted to the
400 cerebellum in humans, but the ectopic expression of this gene has been studied in mouse
401 cortex [5,10], in which it triggers human-like neuronal characteristics, such as an increase in
402 dendritic spine length and density. We therefore suggest that an exploration of human
403 genes/variants specifically associated with the development and functioning of the
404 cerebellum might shed new light on the evolution of human cognition.

405

406 **Limitations**

407 The present results have potential limits in their interpretations. Sources of error in the
408 alignments (e.g. false orthologous, segmental duplications, errors in ancestral sequence
409 reconstruction) are still possible and can result in inflated dN/dS. Moreover, methods to
410 estimate the proteins evolution are expected to give downwardly biased estimates [64].
411 However, our GC12 normalization have already proved to correct for most of those biases in
412 systematic analyses [27] and our raw dN/dS values highly correlate with other independent
413 studies on primates [65]. Moreover, for the enrichment analyses, we used bootstrapping
414 techniques to better control for potential biases induced by differences in GC content and
415 gene length, especially for genes implicated in brain disorders [66]. Finally, our data are
416 openly available on the companion website and allow to check at the variant level which
417 amino acids changed.

Perspectives

Our systematic analysis of protein sequence diversity confirmed that protein-coding genes relating to brain function are among the most highly conserved in the human genome. The set of divergent protein-coding genes identified here may have played specific roles in the evolution of human cognition, by modulating brain size, neuronal migration and/or synaptic physiology, but further genetic and functional studies would shed new light on the role of these divergent genes. Beyond the brain, this resource will be also be useful for estimating the evolutionary pressure acting on genes related to other biological pathways, particularly those displaying signs of positive selection during primate evolution, such as the reproductive and immune systems.

Materials and Methods

Genetic sequences

Alignments with the reference genome: We collected sequences and reconstructed sequence alignments with the reference human genome version hg19 (release 19, GRCh37.p13). For the primate common ancestor sequence, we used the Ensemble 6-way Enredo-Pecan-Ortheus (EPO) [26] multiple alignments v71, related to human (hg19), chimpanzee (panTro4), gorilla (gorGor3), orangutan (ponAbe2), rhesus macaque (rheMac3), and marmoset (calJac3). For the two ancestral hominins, Altai and Denisovan, we integrated variants detected by Castellano and colleagues [67] into the standard hg19 sequence (http://cdna.eva.mpg.de/neandertal/, date of access 2014-07-03). Finally, we used the whole-

441 genome alignment of all the primates used in the 6-EPO from the UCSC website
442 (http://hgdownload.soe.ucsc.edu/downloads.html, access online: August 13th, 2015).

443 **VCF annotation:** We combined the VCF file from Castellano and colleagues [67] with the
444 VCF files generated from the ancestor and primate sequence alignments. The global VCF
445 was annotated with ANNOVAR [68] (version of June 2015), using the following databases:
446 refGene, cytoBand, genomicSuperDups, esp6500siv2_all, 1000g2014oct_all,
447 1000g2014oct_afr, 1000g2014oct_eas, 1000g2014oct_eur, avsnp142, ljb26_all, gerp++elem,
448 popfreq_max, exac03_all, exac03_afr, exac03_amr, exac03_eas, exac03_fin, exac03_nfe,
449 exac03_oth, exac03_sas. We also used the Clinvar database
450 (https://ncbi.nlm.nih.gov/clinvar/, date of access 2016-02-03).

451 **ω_{GC12} calculation**

452 Once all the alignments had been collected, we extracted the consensus coding sequences
453 (CCDS) of all protein-coding genes referenced in Ensembl BioMart Grc37, according to the
454 HGNC (date of access 05/05/2015) and NCBI Consensus CDS protein set (date of access
455 2015-08-10). We calculated the number of non-synonymous mutations N, the number of
456 synonymous mutations S, the ratio of the number of nonsynonymous mutations per non-
457 synonymous site dN, the number of synonymous mutations per synonymous site dS, and their
458 ratio dN/dS —also called ⍰—between all taxa and the ancestor, using the yn00 algorithm
459 implemented in PamL software [69]. We avoided infinite and null results, by calculating a
460 corrected version of dN/dS. If S was null, we set its value to one to avoid having zero as the
461 numerator. The obtained values were validated through the replication of a recent systematic
462 estimation of dN/dS between Homo Sapiens and two great apes [65] (Pan troglodytes and
463 Pongo abelii; Pearson's $r>0.8$, $p<0.0001$; see Fig. S2). Finally, we obtained our ω_{GC12} value
464 by correcting for the GC12 content of the genes with a generalized linear model and by
465 calculating a *Z*-score for each taxon [27]. GC content has been associated with biases in

466 mutation rates, particularly in primates [70] and humans [71]. We retained only the 11667
467 genes with 1:1 orthologs in primates (extracted for GRCh37.p13 with Ensemble Biomart,
468 access online: February 27th, 2017).

469 **Gene sets**

470 We used different gene sets, starting at the tissue level and then focusing on the brain and key
471 pathways. For body tissues, we used Illumina Body Map 2.0 RNA-Seq data, corresponding to
472 16 human tissue types: adrenal, adipose, brain, breast, colon, heart, kidney, liver, lung,
473 lymph, ovary, prostate, skeletal muscle, testes, thyroid, and white blood cells (for more
474 information: https://personal.broadinstitute.org/mgarber/bodymap_schroth.pdf; data
475 preprocessed with Cufflinks, accessed May 5, 2015 at http://cureffi.org). We also used the
476 microarray dataset of Su and colleagues [30] (Human U133A/GNF1H Gene Atlas, accessed
477 May 4, 2015 at http://biogps.org). Finally, we also replicated our results with recent RNAseq
478 data from the GTEx Consortium [31] (https://www.gtexportal.org/home/).

479 For the brain, we used the dataset of Su and colleagues and the Human Protein Atlas data
480 (accessed November 7, 2017 at https://www.proteinatlas.org). For analysis of the biological
481 pathways associated with the brain, we used KEGG (accessed February 25, 2015, at
482 http://www.genome.jp/kegg/), synaptic genes curated by the group of Danielle Posthuma at
483 Vrije Universiteit (accessed September 1, 2014, at https://ctg.cncr.nl/software/genesets), and
484 mass spectrometry data from Loh and colleagues [72]. Finally, for the diseases associated
485 with the brain, we combined gene sets generated from Human Phenotype Ontology (accessed
486 April 5, 2016, at http://human-phenotype-ontology.github.io) and OMIM (accessed April 5,
487 2016, at https://omim.org), and curated lists: the 65 risk genes proposed by Sanders and
488 colleagues [73] (TADA), the candidate genes for autism spectrum disorders from SFARI
489 (accessed July 17, 2015 at https://gene.sfari.org), the Developmental Brain Disorder or DBD
490 (accessed July 12, 2016 at https://geisingeradmi.org/care-innovation/studies/dbd-genes/), and

Cancer Census (accessed November 24, 2016 at cancer.sanger.ac.uk/census) data. Note that the combination of HPO & OMIM is the most exhaustive, making it possible to avoid missing potential candidate genes, but this combination does not identify specific associations.

SynGO was generously provided by Matthijs Verhage (access date: January 11, 2019). This ontology is a consistent, evidence-based annotation of synaptic gene products developed by the SynGO consortium (2015-2017) in collaboration with the GO-consortium. It extends the existing Gene Ontology (GO) of the synapse and follows the same dichotomy between biological processes (BP) and cellular components (CC).

For single-cell transcriptomics datasets, we identified the genes specifically highly expressed in each cell type, following the same strategy as used for the other RNAseq datasets. The single-cell data for the developing human cortex were kindly provided by Maximilian Haeussler (available at https://cells.ucsc.edu; access date: October 30, 2018). The single-cell transcriptional atlas data for the developing murine cerebellum [40] were kindly provided by Robert A. Carter (access date: January 29, 2019). For each cell type, we combined expression values cross all available replicates, to guarantee a high signal-to-noise ratio. We then calculated the values for the associated genes in *Homo sapiens* according to the paralogous correspondence between humans and mice (Ensembl Biomart accessed on February 23, 2019).

Gene nomenclature

We extracted all the EntrezId of the protein-coding genes for Grc37 from Ensembl Biomart. We used the HGNC database to recover their symbols. For the 46 unmapped genes, we searched the NCBI database manually for the official symbol.

514 **McDonald-Kreitman-test (MK) and neutrality index (NI)**

515 We assessed the possible fixation of variants in the *Homo sapiens* population by first
516 calculating the relative ratio of non-synonymous to synonymous polymorphism (pN/pS) from
517 the 1000 Genomes VCF for all SNPs, for SNPs with a minor allele frequency (MAF) <1%
518 and >5%. SNPs were annotated with ANNOVAR across 1000 Genomes Project (ALL+5
519 ethnicity groups), ESP6500 (ALL+2 ethnicity groups), ExAC (ALL+7 ethnicity groups), and
520 CG46 (see http://annovar.openbioinformatics.org/en/latest/user-guide/filter/#popfreqmax-
521 and-popfreqall-annotations for more details). We then performed the McDonald–Kreitman
522 test by calculating the neutrality index (NI) as the ratio of raw pN/pS and dN/dS values [74].
523 We considered the divergent genes to be fixed in the population when NI < 1.

524 **Protein-protein interaction network**

525 We plotted the protein-protein interaction (PPI) network, by combining eight human
526 interactomes: the Human Integrated Protein-Protein Interaction Reference (HIPPIE)
527 (accessed August 10, 2017 at http://cbdm-01.zdv.uni-mainz.de/~mschaefer/hippie/), the
528 Agile Protein Interactomes DataServer (APID) (accessed September 7, 2017 at
529 http://cicblade.dep.usal.es:8080/APID/), CORUM – the comprehensive resource of
530 mammalian protein complexes (accessed July 13, 2017 at http://mips.helmholtz-
531 muenchen.de/corum/), and five PPI networks from of the Center for Cancer Systems Biology
532 (CCSB) (accessed July 12, 2016 at http://interactome.dfci.harvard.edu/index.php?page=home
533): four high-quality binary protein-protein interaction (PPI) networks generated by a
534 systematic primary yeast two-hybrid assay (Y2H): HI-I-05 from Rual and colleagues [75],
535 Venkatesan-09 from Venkatesan and colleagues [76], Yu-11 from Yu and colleagues [77]
536 and HI-II-14 from Rolland and colleagues [78], plus one high-quality binary literature dataset
537 (Lit-BM-13) from Rolland and colleagues [78], comprising all PPIs that are binary and
538 supported by at least two traceable pieces of evidence (publications and/or methods).

539 **NeuroVault analyses**

540 We used the NeuroVault website [44] to collect 19,244 brain imaging results from fMRI-
541 BOLD studies (*T* and *Z* score maps) and their correlation with the gene expression data [46]
542 of the Allen Brain atlas [45]. The gene expression data of the Allen Brain atlas were
543 normalized and projected into the MNI152 stereotactic space used by NeuroVault, using the
544 spatial coordinates provided by the Allen Brain Institute. An inverse relationship between
545 cortical and subcortical expression dominated the pattern of expression for many genes. We
546 therefore calculated the correlations for the cortex and subcortical structures separately.

547 **Allen Brain data**

548 We downloaded the Allen Brain atlas microarray-based gene data from the Allen Brain
549 website (accessed January 19, 2018 at http://www.brain-map.org). Microarray data were
550 available for six adult brains; the right hemisphere was missing for three donors so we
551 considered only the left hemisphere for our analyses. For each donor, we averaged probes
552 targeting the same gene and falling in the same brain area. We then subjected the data to log
553 normalization and calculated *Z*-scores: across the 20787 genes for each brain region to obtain
554 expression levels; across the 212 brain areas for each gene to obtain expression specificity.
555 For genes with more than one probe, we averaged the normalized values over all probes
556 available. As a complementary dataset, we also used a mapping of the Allen Brain Atlas onto
557 the 68 brain regions of the Freesurfer atlas [79] (accessed April 4, 2017 at
558 https://figshare.com/articles/A_FreeSurfer_view_of_the_cortical_transcriptome_generated_fr
559 om_the_Allen_Human_Brain_Atlas/1439749).

560 **Statistics**

561 **Enrichment analyses:** We first calculated a two-way hierarchical clustering on the
562 normalized dN/dS values (ω_{GC}) across the whole genome (see Fig. 1b; note: 11,667 genes

were included in the analysis to ensure medium-quality coverage for *Homo sapiens*, Neanderthals, Denisovans, and *Pan troglodytes*; see Supplementary table 2). According to 30 clustering indices [80], the best partitioning in terms of evolutionary pressure was into two clusters of genes: constrained (*N*=4825; in HS, mean=-0.88 median=-0.80 SD=0.69) and divergent (N=6842; in HS, mean=0.60 median=0.48 sd=0.63. For each cluster, we calculated the enrichment in biological functions in Cytoscape [81] with the BINGO plugin [82]. We used all 12,400 genes as the background. We eliminated redundancy, by first filtering out all the statistically significant Gene Ontology (GO) terms associated with fewer than 10 or more than 1000 genes, and then combining the remaining genes with the EnrichmentMap plugin [83]. We used a *P*-value cutoff of 0.005, an FDR Q-value cutoff of 0.05, and a Jaccard coefficient of 0.5.

For the cell type-specific expression Aanalysis (CSEA; 86), we used the CSEA method with the online tool http://genetics.wustl.edu/jdlab/csea-tool-2/. This method associates gene lists with brain expression profiles across cell types, regions, and time periods.

Wilcoxon and rank-biserial correlation: We investigated the extent to which each gene set was significantly more conserved or divergent than expected by chance, by performing Wilcoxon tests on the normalized dN/dS values (ω_{GC}) for the genes in the set against zero (the mean value for the genome). We quantified effect size by matched pairs rank-biserial correlation, as described by Kerby [85]. Following non-parametric Wilcoxon signed-rank tests, the rank-biserial correlation was evaluated as the difference between the proportions of negative and positive ranks over the total sum of ranks:

$$rc = \frac{\sum r_+ - \sum r_-}{\sum r_+ + \sum r_-} = f - u$$

It corresponds to the difference between the proportion of observations consistent with the hypothesis (f) minus the proportion of observations contradicting the hypothesis (u), thus

representing an effect size. Like other correlational measures, its value ranges from minus one to plus one, with a value of zero indicating no relationship. In our case, a negative rank-biserial correlation corresponds to a gene set in which more genes have negative ω_{GC} values than positive values, revealing a degree of conservation greater than the mean for all genes (i.e. $\omega_{GC} = 0$). Conversely, a positive rank-biserial correlation corresponds to a gene set that is more divergent than expected by chance (i.e. taking randomly the same number of genes across the whole genome; correction for the potential biases for GC content and CDS length are done at the bootstrap level). All statistics relating to Figures 1d, 2a and 2b are summarized in Supplementary table 3.

Validation by resampling: We also used bootstrapping to correct for potential bias in the length of the coding sequence or the global specificity of gene expression (Tau, see the methods from Kryuchkova-Mostacci and Robinson-Rechavi in [86]). For each of the 10000 permutations, we randomly selected the same number of genes as for the sample of genes from the total set of genes for which dN/dS was not missing. We corrected for CCDS length and GC content by bootstrap resampling. We estimated significance, to determine whether the null hypothesis could be rejected, by calculating the number of bootstrap draws (B_i) falling below and above the observed measurement (m). The related empirical *p*-value was calculated as follows:

$$p = 2 * \min\left(\frac{1 + \sum_i B_i \geq m}{N + 1}, \frac{1 + \sum_i B_i \leq m}{N + 1}\right)$$

Data & code availability: All the data and code supporting the findings of this study are available from our resource website: http://neanderthal.pasteur.fr

606

607 **Acknowledgments**

608 We thank J-P. Changeux, L. Quintana-Murci, E. Patin, G. Laval, B. Arcangioli, D.
609 DiGregorio, L. Bally-Cuif, A. Chedotal, C. Berthelot, H. Roest Crollius, and V. Warrier for
610 advice and comments, and the members of the Human Genetics and Cognitive Functions
611 laboratory for helpful discussions. We also thank C. Gorgolewski, R. Carter, M. Haeussler,
612 M. Verhage and the SynGO consortium for providing key datasets without which this work
613 would not have been possible. This work was supported by the Institut Pasteur; *Centre*
614 *National de la Recherche Scientifique*; Paris Diderot University; the *Fondation pour la*
615 *Recherche Médicale* [DBI20141231310]; the Human Brain Project; the Cognacq-Jay
616 Foundation; the Bettencourt-Schueller Foundation; and the *Agence Nationale de la*
617 *Recherche* (ANR) [SynPathy]. This research was supported by the Laboratory of Excellence
618 GENMED (Medical Genomics) grant no. ANR-10-LABX-0013, Bio-Psy and by the
619 INCEPTION program ANR-16-CONV-0005, all managed by the ANR part of the
620 Investments for the Future program. The funders had no role in study design, data collection
621 and analysis, the decision to publish, or preparation of the manuscript.

622

623 **Author contributions**

624 G.D. and T.B. devised the project and came up with the main conceptual ideas. G.D.
625 developed the methods, performed the analyses, and designed the figures. G.D. and T.B.
626 discussed the results and wrote the manuscript. S.M. developed the companion website.

627

628 **References**

629 1. Dunbar RIM, Shultz S. Why are there so many explanations for primate brain evolution?
630 Phil Trans R Soc B. 2017;372: 20160244. doi:10.1098/rstb.2016.0244

631 2. Varki A, Geschwind DH, Eichler EE. Human uniqueness: genome interactions with
632 environment, behaviour and culture. Nat Rev Genet. 2008;9: nrg2428.
633 doi:10.1038/nrg2428

634 3. Neubauer S, Hublin J-J, Gunz P. The evolution of modern human brain shape. Sci Adv.
635 2018;4: eaao5961. doi:10.1126/sciadv.aao5961

636 4. Balsters JH, Cussans E, Diedrichsen J, Phillips KA, Preuss TM, Rilling JK, et al.
637 Evolution of the cerebellar cortex: the selective expansion of prefrontal-projecting
638 cerebellar lobules. NeuroImage. 2010;49: 2045–2052.
639 doi:10.1016/j.neuroimage.2009.10.045

640 5. Charrier C, Joshi K, Coutinho-Budd J, Kim J-E, Lambert N, de Marchena J, et al.
641 Inhibition of SRGAP2 Function by Its Human-Specific Paralogs Induces Neoteny
642 during Spine Maturation. Cell. 2012;149: 923–935. doi:10.1016/j.cell.2012.03.034

643 6. Florio M, Albert M, Taverna E, Namba T, Brandl H, Lewitus E, et al. Human-specific
644 gene ARHGAP11B promotes basal progenitor amplification and neocortex expansion.
645 Sci N Y NY. 2015;347: 1–9. doi:10.1126/science.aaa1975

646 7. Suzuki IK, Gacquer D, Van Heurck R, Kumar D, Wojno M, Bilheu A, et al. Human-
647 Specific NOTCH2NL Genes Expand Cortical Neurogenesis through Delta/Notch
648 Regulation. Cell. 2018;173: 1370-1384.e16. doi:10.1016/j.cell.2018.03.067

649 8. Dennis MY, Harshman L, Nelson BJ, Penn O, Cantsilieris S, Huddleston J, et al. The
650 evolution and population diversity of human-specific segmental duplications. Nat Ecol
651 Evol. 2017;1: 69. doi:10.1038/s41559-016-0069

652 9. Nuttle X, Giannuzzi G, Duyzend MH, Schraiber JG, Narvaiza I, Sudmant PH, et al.
653 Emergence of a Homo sapiens-specific gene family and chromosome 16p11.2 CNV
654 susceptibility. Nature. 2016;536: 205–209. doi:10.1038/nature19075

655 10. Dennis MY, Nuttle X, Sudmant PH, Antonacci F, Graves TA, Nefedov M, et al.
656 Evolution of Human-Specific Neural SRGAP2 Genes by Incomplete Segmental
657 Duplication. Cell. 2012;149: 912–922. doi:10.1016/j.cell.2012.03.033

658 11. Enard W, Przeworski M, Fisher SE, Lai CSL, Wiebe V, Kitano T, et al. Molecular
659 evolution of FOXP2, a gene involved in speech and language. Nature. 2002;418: 869–
660 872. doi:10.1038/nature01025

661 12. Montgomery SH, Mundy NI, Barton RA. ASPM and mammalian brain evolution: a case
662 study in the difficulty in making macroevolutionary inferences about gene-phenotype
663 associations. Proc R Soc B Biol Sci. 2014;281: 20131743. doi:10.1098/rspb.2013.1743

664 13. Enard W, Gehre S, Hammerschmidt K, Hölter SM, Blass T, Somel M, et al. A humanized
665 version of Foxp2 affects cortico-basal ganglia circuits in mice. Cell. 2009;137: 961–
666 971. doi:10.1016/j.cell.2009.03.041

14. Atkinson EG, Audesse AJ, Palacios JA, Bobo DM, Webb AE, Ramachandran S, et al. No Evidence for Recent Selection at FOXP2 among Diverse Human Populations. Cell. 2018;0. doi:10.1016/j.cell.2018.06.048

15. Miyata T, Kuma K, Iwabe N, Nikoh N. A possible link between molecular evolution and tissue evolution demonstrated by tissue specific genes. Idengaku Zasshi. 1994;69: 473–480.

16. Wang H-Y, Chien H-C, Osada N, Hashimoto K, Sugano S, Gojobori T, et al. Rate of Evolution in Brain-Expressed Genes in Humans and Other Primates. PLoS Biol. 2006;5: e13. doi:10.1371/journal.pbio.0050013

17. Tuller T, Kupiec M, Ruppin E. Evolutionary rate and gene expression across different brain regions. Genome Biol. 2008;9: R142. doi:10.1186/gb-2008-9-9-r142

18. King M-C, Wilson AC. Evolution at two levels in humans and chimpanzees. Science. 1975;188: 107–116. doi:10.1126/science.1090005

19. Pollard KS, Salama SR, Lambert N, Lambot M-A, Coppens S, Pedersen JS, et al. An RNA gene expressed during cortical development evolved rapidly in humans. Nature. 2006;443: 167–172. doi:10.1038/nature05113

20. Changeux J-P. Climbing Brain Levels of Organisation from Genes to Consciousness. Trends Cogn Sci. 2017;21: 168–181. doi:10.1016/j.tics.2017.01.004

21. Calarco JA, Xing Y, Cáceres M, Calarco JP, Xiao X, Pan Q, et al. Global analysis of alternative splicing differences between humans and chimpanzees. Genes Dev. 2007;21: 2963–2975. doi:10.1101/gad.1606907

22. Sundaram L, Gao H, Padigepati SR, McRae JF, Li Y, Kosmicki JA, et al. Predicting the clinical impact of human mutation with deep neural networks. Nat Genet. 2018 [cited 24 Jul 2018]. doi:10.1038/s41588-018-0167-z

23. Havrilla JM, Pedersen BS, Layer RM, Quinlan AR. A map of constrained coding regions in the human genome. Nat Genet. 2019;51: 88. doi:10.1038/s41588-018-0294-6

24. Dorus S, Vallender EJ, Evans PD, Anderson JR, Gilbert SL, Mahowald M, et al. Accelerated Evolution of Nervous System Genes in the Origin of Homo sapiens. Cell. 2004;119: 1027–1040. doi:10.1016/j.cell.2004.11.040

25. Huang Y, Xie C, Ye AY, Li C-Y, Gao G, Wei L. Recent Adaptive Events in Human Brain Revealed by Meta-Analysis of Positively Selected Genes. Robinson-Rechavi M, editor. PLoS ONE. 2013;8: e61280. doi:10.1371/journal.pone.0061280

26. Paten B, Herrero J, Beal K, Fitzgerald S, Birney E. Enredo and Pecan: Genome-wide mammalian consistency-based multiple alignment with paralogs. Genome Res. 2008;18: 1814–1828. doi:10.1101/gr.076554.108

27. Kapheim KM, Pan H, Li C, Salzberg SL, Puiu D, Magoc T, et al. Genomic signatures of evolutionary transitions from solitary to group living. Science. 2015;348: 1139–1143. doi:10.1126/science.aaa4788

28. Yang Z, Bielawski J. Statistical methods for detecting molecular adaptation. Trends Ecol Evol. 2000;15: 496–503. doi:10.1016/s0169-5347(00)01994-7

29. O'Toole ÁN, Hurst LD, McLysaght A. Faster Evolving Primate Genes Are More Likely to Duplicate. Mol Biol Evol. 2018;35: 107–118. doi:10.1093/molbev/msx270

30. Su AI, Wiltshire T, Batalov S, Lapp H, Ching KA, Block D, et al. A gene atlas of the mouse and human protein-encoding transcriptomes. Proc Natl Acad Sci U S A. 2004;101: 6062–6067. doi:10.1073/pnas.0400782101

31. Consortium TGte. The Genotype-Tissue Expression (GTEx) pilot analysis: Multitissue gene regulation in humans. Science. 2015;348: 648–660. doi:10.1126/science.1262110

32. Schoenemann PT, Sheehan MJ, Glotzer LD. Prefrontal white matter volume is disproportionately larger in humans than in other primates. Nat Neurosci. 2005;8: 242–252. doi:10.1038/nn1394

33. Frith C, Dolan R. The role of the prefrontal cortex in higher cognitive functions. Cogn Brain Res. 1996;5: 175–181. doi:10.1016/S0926-6410(96)00054-7

34. Tao X, West AE, Chen WG, Corfas G, Greenberg ME. A calcium-responsive transcription factor, CaRF, that regulates neuronal activity-dependent expression of BDNF. Neuron. 2002;33: 383–395.

35. Whitney O, Pfenning AR, Howard JT, Blatti CA, Liu F, Ward JM, et al. Core and region-enriched networks of behaviorally regulated genes and the singing genome. Science. 2014;346: 1256780. doi:10.1126/science.1256780

36. Ruano D, Abecasis GR, Glaser B, Lips ES, Cornelisse LN, de Jong APH, et al. Functional Gene Group Analysis Reveals a Role of Synaptic Heterotrimeric G Proteins in Cognitive Ability. Am J Hum Genet. 2010;86: 113–125. doi:10.1016/j.ajhg.2009.12.006

37. Lips ES, Cornelisse LN, Toonen RF, Min JL, Hultman CM, Holmans PA, et al. Functional gene group analysis identifies synaptic gene groups as risk factor for schizophrenia. Mol Psychiatry. 2012;17: 996–1006.

38. Miller JA, Ding S-L, Sunkin SM, Smith KA, Ng L, Szafer A, et al. Transcriptional landscape of the prenatal human brain. Nature. 2014;508: 199–206. doi:10.1038/nature13185

39. Brazel CY, Romanko MJ, Rothstein RP, Levison SW. Roles of the mammalian subventricular zone in brain development. Prog Neurobiol. 2003;69: 49–69. doi:10.1016/S0301-0082(03)00002-9

40. Carter RA, Bihannic L, Rosencrance C, Hadley JL, Tong Y, Phoenix TN, et al. A Single-Cell Transcriptional Atlas of the Developing Murine Cerebellum. Curr Biol. 2018;28: 2910-2920.e2. doi:10.1016/j.cub.2018.07.062

41. Nowakowski TJ, Bhaduri A, Pollen AA, Alvarado B, Mostajo-Radji MA, Lullo ED, et al. Spatiotemporal gene expression trajectories reveal developmental hierarchies of the human cortex. Science. 2017;358: 1318–1323. doi:10.1126/science.aap8809

42. Lein ES, Hawrylycz MJ, Ao N, Ayres M, Bensinger A, Bernard A, et al. Genome-wide atlas of gene expression in the adult mouse brain. Nature. 2007;445: 168–176. doi:10.1038/nature05453

747 43. Coene KLM, Roepman R, Doherty D, Afroze B, Kroes HY, Letteboer SJF, et al. OFD1 is
748 mutated in X-linked Joubert syndrome and interacts with LCA5-encoded lebercilin. Am
749 J Hum Genet. 2009;85: 465–481. doi:10.1016/j.ajhg.2009.09.002

750 44. Gorgolewski KJ, Varoquaux G, Rivera G, Schwarz Y, Ghosh SS, Maumet C, et al.
751 NeuroVault.org: a web-based repository for collecting and sharing unthresholded
752 statistical maps of the human brain. Front Neuroinformatics. 2015;9: 8.
753 doi:10.3389/fninf.2015.00008

754 45. Hawrylycz MJ, Lein ES, Guillozet-Bongaarts AL, Shen EH, Ng L, Miller JA, et al. An
755 anatomically comprehensive atlas of the adult human brain transcriptome. Nature.
756 2012;489: 391–399. doi:10.1038/nature11405

757 46. Gorgolewski KJ, Fox AS, Chang L, Schäfer A, Arélin K, Burmann I, et al. Tight fitting
758 genes: finding relations between statistical maps and gene expression patterns.
759 F1000Research. 2014;5. doi:10.7490/f1000research.1097120.1

760 47. Karayannis T, Au E, Patel JC, Kruglikov I, Markx S, Delorme R, et al. Cntnap4
761 differentially contributes to GABAergic and dopaminergic synaptic transmission.
762 Nature. 2014;511: 236–240. doi:10.1038/nature13248

763 48. Jamain S, Quach H, Betancur C, Råstam M, Colineaux C, Gillberg IC, et al. Mutations of
764 the X-linked genes encoding neuroligins NLGN3 and NLGN4 are associated with
765 autism. Nat Genet. 2003;34: 27–29. doi:10.1038/ng1136

766 49. Abrahams BS, Arking DE, Campbell DB, Mefford HC, Morrow EM, Weiss LA, et al.
767 SFARI Gene 2.0: a community-driven knowledgebase for the autism spectrum disorders
768 (ASDs). Mol Autism. 2013;4: 36. doi:10.1186/2040-2392-4-36

769 50. Mejias R, Adamczyk A, Anggono V, Niranjan T, Thomas GM, Sharma K, et al. Gain-of-
770 function glutamate receptor interacting protein 1 variants alter GluA2 recycling and
771 surface distribution in patients with autism. Proc Natl Acad Sci U S A. 2011;108: 4920–
772 4925. doi:10.1073/pnas.1102233108

773 51. Paracchini S, Thomas A, Castro S, Lai C, Paramasivam M, Wang Y, et al. The
774 chromosome 6p22 haplotype associated with dyslexia reduces the expression of
775 KIAA0319, a novel gene involved in neuronal migration. Hum Mol Genet. 2006;15:
776 1659–1666. doi:10.1093/hmg/ddl089

777 52. Franquinho F, Nogueira-Rodrigues J, Duarte JM, Esteves SS, Carter-Su C, Monaco AP,
778 et al. The Dyslexia-susceptibility Protein KIAA0319 Inhibits Axon Growth Through
779 Smad2 Signaling. Cereb Cortex N Y N 1991. 2017;27: 1732–1747.
780 doi:10.1093/cercor/bhx023

781 53. Dennis MY, Eichler EE. Human adaptation and evolution by segmental duplication. Curr
782 Opin Genet Dev. 2016;41: 44–52. doi:10.1016/j.gde.2016.08.001

783 54. Hayward P. Joubert syndrome may provide clues about human evolution. Lancet Neurol.
784 2004;3: 574. doi:10.1016/S1474-4422(04)00870-1

785 55. Mekel-Bobrov N, Gilbert SL, Evans PD, Vallender EJ, Anderson JR, Hudson RR, et al.
786 Ongoing adaptive evolution of ASPM, a brain size determinant in Homo sapiens.
787 Science. 2005;309: 1720–1722. doi:10.1126/science.1116815

788 56. Evans PD, Gilbert SL, Mekel-Bobrov N, Vallender EJ, Anderson JR, Vaez-Azizi LM, et
789 al. Microcephalin, a gene regulating brain size, continues to evolve adaptively in
790 humans. Science. 2005;309: 1717–1720. doi:10.1126/science.1113722

791 57. Yu F, Hill RS, Schaffner SF, Sabeti PC, Wang ET, Mignault AA, et al. Comment on
792 "Ongoing adaptive evolution of ASPM, a brain size determinant in Homo sapiens."
793 Science. 2007;316: 370. doi:10.1126/science.1137568

794 58. Unger S, Górna MW, Le Béchec A, Do Vale-Pereira S, Bedeschi MF, Geiberger S, et al.
795 FAM111A mutations result in hypoparathyroidism and impaired skeletal development.
796 Am J Hum Genet. 2013;92: 990–995. doi:10.1016/j.ajhg.2013.04.020

797 59. Hoischen A, van Bon BWM, Rodríguez-Santiago B, Gilissen C, Vissers LELM, de Vries
798 P, et al. De novo nonsense mutations in ASXL1 cause Bohring-Opitz syndrome. Nat
799 Genet. 2011;43: 729–731. doi:10.1038/ng.868

800 60. Ferland RJ, Eyaid W, Collura RV, Tully LD, Hill RS, Al-Nouri D, et al. Abnormal
801 cerebellar development and axonal decussation due to mutations in AHI1 in Joubert
802 syndrome. Nat Genet. 2004;36: 1008–1013. doi:10.1038/ng1419

803 61. Gould DB, Walter MA. Mutational analysis of BARHL1 and BARX1 in three new
804 patients with Joubert syndrome. Am J Med Genet A. 2004;131: 205–208.
805 doi:10.1002/ajmg.a.30227

806 62. Koziol LF, Budding DE, Chidekel D. From movement to thought: executive function,
807 embodied cognition, and the cerebellum. Cerebellum Lond Engl. 2012;11: 505–525.
808 doi:10.1007/s12311-011-0321-y

809 63. Rao SM, Mayer AR, Harrington DL. The evolution of brain activation during temporal
810 processing. Nat Neurosci. 2001;4: 317–323. doi:10.1038/85191

811 64. Eyre-Walker A, Keightley PD. Estimating the Rate of Adaptive Molecular Evolution in
812 the Presence of Slightly Deleterious Mutations and Population Size Change. Mol Biol
813 Evol. 2009;26: 2097–2108. doi:10.1093/molbev/msp119

814 65. Biswas K, Chakraborty S, Podder S, Ghosh TC. Insights into the dN/dS ratio
815 heterogeneity between brain specific genes and widely expressed genes in species of
816 different complexity. Genomics. 2016;108: 11–17. doi:10.1016/j.ygeno.2016.04.004

817 66. Zylka MJ, Simon JM, Philpot BD. Gene length matters in neurons. Neuron. 2015;86:
818 353–355. doi:10.1016/j.neuron.2015.03.059

819 67. Castellano S, Parra G, Sanchez-Quinto FA, Racimo F, Kuhlwilm M, Kircher M, et al.
820 Patterns of coding variation in the complete exomes of three Neandertals. Proc Natl
821 Acad Sci U S A. 2014;111: 6666–6671. doi:10.1073/pnas.1405138111

822 68. Wang K, Li M, Hakonarson H. ANNOVAR: functional annotation of genetic variants
823 from high-throughput sequencing data. Nucleic Acids Res. 2010;38: e164–e164.
824 doi:10.1093/nar/gkq603

825 69. Yang Z. PAML 4: Phylogenetic Analysis by Maximum Likelihood. Mol Biol Evol.
826 2007;24: 1586–1591. doi:10.1093/molbev/msm088

827 70. Galtier N, Duret L, Glémin S, Ranwez V. GC-biased gene conversion promotes the
828 fixation of deleterious amino acid changes in primates. Trends Genet. 2009;25: 1–5.

829 71. Kostka D, Hubisz MJ, Siepel A, Pollard KS. The Role of GC-Biased Gene Conversion in
830 Shaping the Fastest Evolving Regions of the Human Genome. Mol Biol Evol. 2012;29:
831 1047–1057. doi:10.1093/molbev/msr279

832 72. Loh KH. Proteomics: The proteomes of excitatory and inhibitory synaptic clefts. Nat
833 Methods. 2016;13: 903–903. doi:10.1038/nmeth.4050

834 73. Sanders SJ, He X, Willsey AJ, Ercan-Sencicek AG, Samocha KE, Cicek AE, et al.
835 Insights into Autism Spectrum Disorder Genomic Architecture and Biology from 71
836 Risk Loci. Neuron. 2015;87: 1215–1233. doi:10.1016/j.neuron.2015.09.016

837 74. McDonald JH, Kreitman M. Adaptive protein evolution at the Adh locus in Drosophila.
838 Nature. 1991;351: 351652a0. doi:10.1038/351652a0

839 75. Rual J-F, Venkatesan K, Hao T, Hirozane-Kishikawa T, Dricot A, Li N, et al. Towards a
840 proteome-scale map of the human protein-protein interaction network. Nature.
841 2005;437: 1173–1178. doi:10.1038/nature04209

842 76. Venkatesan K, Rual J-F, Vazquez A, Stelzl U, Lemmens I, Hirozane-Kishikawa T, et al.
843 An empirical framework for binary interactome mapping. Nat Methods. 2009;6: 83–90.
844 doi:10.1038/nmeth.1280

845 77. Yu H, Tardivo L, Tam S, Weiner E, Gebreab F, Fan C, et al. Next-generation sequencing
846 to generate interactome datasets. Nat Methods. 2011;8: 478–480.
847 doi:10.1038/nmeth.1597

848 78. Rolland T, Taşan M, Charloteaux B, Pevzner SJ, Zhong Q, Sahni N, et al. A proteome-
849 scale map of the human interactome network. Cell. 2014;159: 1212–1226.
850 doi:10.1016/j.cell.2014.10.050

851 79. French L. A FreeSurfer view of the cortical transcriptome generated from the Allen
852 Human Brain Atlas. 2017. doi:10.6084/m9.figshare.1439749.v11

853 80. Charrad M, Ghazzali N, Boiteau V, Niknafs A. NbClust: an R package for determining
854 the relevant number of clusters in a data set. J Stat Softw. 2014;61: 1–36.

855 81. Shannon P, Markiel A, Ozier O, Baliga NS, Wang JT, Ramage D, et al. Cytoscape: A
856 Software Environment for Integrated Models of Biomolecular Interaction Networks.
857 Genome Res. 2003;13: 2498–2504. doi:10.1101/gr.1239303

858 82. Maere S, Heymans K, Kuiper M. BiNGO: a Cytoscape plugin to assess
859 overrepresentation of gene ontology categories in biological networks. Bioinforma Oxf
860 Engl. 2005;21: 3448–3449. doi:10.1093/bioinformatics/bti551

861 83. Merico D, Isserlin R, Stueker O, Emili A, Bader GD. Enrichment Map: A Network-
862 Based Method for Gene-Set Enrichment Visualization and Interpretation. PLOS ONE.
863 2010;5: e13984. doi:10.1371/journal.pone.0013984

864 84. Xu X, Wells AB, O'Brien DR, Nehorai A, Dougherty JD. Cell Type-Specific Expression
865 Analysis to Identify Putative Cellular Mechanisms for Neurogenetic Disorders. J
866 Neurosci. 2014;34: 1420–1431. doi:10.1523/JNEUROSCI.4488-13.2014

867 85. Kerby DS. The Simple Difference Formula: An Approach to Teaching Nonparametric
868 Correlation. Compr Psychol. 2014;3: 11.IT.3.1. doi:10.2466/11.IT.3.1

869 86. Kryuchkova-Mostacci N, Robinson-Rechavi M. A benchmark of gene expression tissue-
870 specificity metrics. Brief Bioinform. 2016; bbw008. doi:10.1093/bib/bbw008